BII-2 THE FRACTURE OF POLYCRYSTALLINE IRON*

C. J. McMahon, Jr.+ and Morris Cohen++

ABSTRACT

The results of recent microstructural research on the cleavage, intergranular, and ductile modes of fracture in polycyrstalline iron are presented. Various possible mechanisms of cleavage initiation are examined and the importance of carbide cracking in this connection is demonstrated. The conditions for cleavage fracture are analyzed in terms of the relative probabilities of crack initiation and long-range crack propagation. The effects of carbide cracking on the ductile-brittle transition temperature, T_d, are considered, and the physical significance of T_d itself is discussed. Finally, the role of carbon distribution in the tendency toward intergranular fracture is described.

1. Introduction

At the Swampscott Conference on Fracture in 1959, Hahn et al. (1) presented the results of a comprehensive investigation of brittle fracture in iron and steel as carried out at M.I.T. over a period of years. The research to be described in the present paper was motivated by this previous work, and is focused on the microstructural aspects of fracture in polycrystalline ferrite. The micromechanisms of initiation and propagation of transcrystalline cleavage, as well as of intergranular and ductile rupture, are summarized here in order to provide a self-consistent picture of the fracture behavior of this material.

---

*This paper is based on research sponsored at the Massachusetts Institute of Technology by the Ship Structure Committee, Washington, D.C., and at the University of Pennsylvania by the Advanced Research Projects Agency, Washington, D.C.

+School of Metallurgical Engineering and Laboratory for Research on the Structure of Matter, University of Pennsylvania, Philadelphia, Pa., formerly in the Department of Metallurgy, Massachusetts Institute of Technology, Cambridge, Massachusetts.

++Department of Metallurgy, Massachusetts Institute of Technology, Cambridge, Massachusetts.

2. Initiation of Cleavage

Following the now-classical generalized model proposed by Zener (2) for the initiation of fracture by plastic deformation, much attention was directed during the 1950's toward various ways in which dislocation pileups could lead to cleavage in b.c.c. metals (3,4,5). In the past several years, metallographic research along these lines, mainly on single crystals, has demonstrated that cleavage can be initiated at twin intersections, (6, 7) slip-band intersections, (7) and at the intersections of twins with grain boundaries (8). The intersections of slip bands with each other and with grain boundaries can be important in the nucleation of cleavage in nonmetallic crystals and polycrystals (9).

Studies of cleavage in single crystals have produced rather clear-cut results, because in this case it is often possible to determine the fracture origin by examination of the fracture surface and to identify the initiation mechanism by the deformation markings. Similarly directed research in polycrystals has usually proved less successful, because it is quite difficult to locate unambiguously the fracture origin, except in very coarse-grained specimens, and there is further uncertainty in establishing the initiating mechanism even if the point of origin can be found. As a result, proposed mechanisms are often deduced from considerations of the stress-strain curves or the behavior of fracture stress as a function of temperature, or by inference from mechanisms observed in single crystals. However, a more straightforward approach to the problem of cleavage initiation in polycrystals is to examine incipient fractures in the form of arrested cleavage microcracks, which can be found under proper conditions in many systems. This approach to the study of brittle fracture of iron and steel was introduced by Low (10) and carried forward by Hahn et al. (1).

We have found that certain generalizations about the dominant mechanisms of cleavage initiation in iron can be arrived at by examining the appearance and behavior of a large number of cleavage microcracks on the surface and in the interior of tensile specimens tested at various temperatures. Such a program has been carried out using two vacuum-melted ferrites, designated F4 and F5, whose compositions, heat treatments, and grain sizes are given in Table 1. The experimental details have been described elsewhere (11). Briefly, the materials were rather coarse grained and contained Fe_3C particles lying mainly along grain boundaries. The carbides in F4 were naturally larger and more numerous than in F5. Tensile tests were performed on flat specimens ($1\frac{9}{16} \times \frac{1}{4} \times \frac{1}{8}$ inch gauge section) at temperatures between ambient and liquid nitrogen. Extensive metallographic examinations were performed both on fractured specimens and on replicas made during interrupted tensile tests.

During the early stages of the present investigations, cleavage-initiation mechanisms involving slip and twin intersections were under very active consideration, and our primary goal was to evaluate the relative importance of these two possibilities in the case of polycrystalline iron. However, it had been long established, but seldom recalled, that the cracking of carbides can initiate cleavage in iron (12,13) and for this reason we decided to delineate the role of carbides in the overall brittle-fracture problem.

The experimental evidence on this question demonstrated convincingly that the influence of the grain-boundary carbides almost completely overshadows that of twin and slip-band intersections in these materials (11). When polycrystalline specimens are tested at temperatures below the ductile-brittle transition, T_d, microcleavage cracks appear in the ferrite grains after plastic yielding, and become more numerous with increasing plastic strain.* Fracture finally occurs by either the unarrested propagation of a newly-formed microcrack or the reactivation of one formed earlier. The total amount of plastic strain decreases with testing temperature to less than one percent at -195°C. Here, very few (if any) microcracks are found in the specimen, indicating that the first, or one of the first, microcracks propagates to ultimate failure.

Typically, of all the ferrite microcracks observed on the side faces of fractured tensile specimens, about 20 percent were obviously associated with cracks in carbides, as shown in Fig. 1. The carbide platelet in the grain boundary was cracked by one of the twins which struck it during plastic deformation, giving rise to the ferrite microcrack in the next grain. Fig. 2. contains a set of photomicrographs taken from the same location on the side face of an F4 specimen, tensile tested in three steps at -180°C according to the stress-strain curves in Fig. 3. The microcrack BB' in Fig. 2b was one of 17 new microcracks formed during the second loading step. It was initiated by a crack in the grain-boundary carbide at B and was then arrested by the opposite grain boundary at B'.

To determine the origin of the microcracks not associated with carbides on the surface, the specimens were sectioned progressively by grinding and repolishing, thus providing a three-dimensional view of the microstructures. In almost all instances, the microcracks in the F4 material were found to originate at cracked carbides inside the specimen, if not at the surface. An example of the interior case is given in Fig. 4. In the F5 ferrite, the sectioning results were less conclusive, probably due to the fineness of the

---

* Microcracks also form at test temperature above T_d, but this case is considered in a later section.

carbides and the greater chance of skipping carbides between the sectioned layers. Nevertheless, at least the majority of the microcrack sources in the F5 ferrite were definitely traced to cracked carbides.

A summary of crack-source observations supporting the above statements is given in Table II. The increase in the microcrack density with plastic strain in these ferrites is shown in Figure 5. However, this effect of strain appears to saturate, presumably because the more efficient crack sources are used up.

A comparison between the microcracking tendency and tensile behavior of F4 and F5 ferrite is shown in Fig. 6. These curves will be discussed in more detail in the next section, but at this point the maximum in microcrack density, which occurs at a temperature below T_d in both materials, should be noted.

This maximum is also observed in mild steel (1), and results from two conflicting effects. As the test temperature is lowered, the tendency for microcracks to nucleate at cracked carbides increases because of the greater resistance to dislocation motion that would otherwise permit yielding of the ferrite at the ferrite-cementite interface. Thus, aside from the effect of an increase in plastic strain, which causes more carbides to crack at any given temperature (Fig. 5), the probability of microcrack formation is enhanced due to lowering of the test temperature. The latter factor controls the observed microcrack density in specimens fractured in the range of temperatures above the maximum in the microcracking curve. At test temperatures below this range, the propagation process begins to be favored sufficiently so as to severely limit the overall strain to ultimate fracture, and the microcrack density in fractured specimens then decreases with decreasing temperature.

The significance of these results can be summarized as follows:

(1) Since microcracks in these polycrystalline ferrites form in increasing numbers during the strain-hardening portion of the stress-strain curve and are not associated with the discontinuous yielding stage, dislocation pileup models for crack initiation (4, 5), which predict crack formation during yielding, are not applicable here.

(2) Twin intersections, which can play a dominant role in cleavage initiation in single crystals (6, 7) and in very coarse-grained polycrystals of b.c.c. metals (14), are not important in the present materials, at least at temperatures above -195°C. This point is further emphasized when the similar twinning behavior of the two ferritic materials (Fig. 7) is contrasted with their greatly dissimilar microcracking tendencies. (Fig. 6).

Perhaps if the grain size were further coarsened, or if higher strain rates or lower test temperatures were used, twin intersections would assume more importance. It appears that, under the test

conditions adopted for these studies, the grain size is not coarse enough to allow twins to achieve sufficient velocity and thickness to nucleate cleavage before plastic relaxation occurs.

In the absence of carbides or carbide cracking, it may be expected that some other mechanism, such as twin or slip-band intersections, would operate to induce cleavage at higher stresses. This would become especially true in the presence of strong solid-solution hardening elements, e.g., silicon or phosphorus, because even if carbides are present, they do not crack until plastic deformation of the surrounding ferrite takes place. Thus, as the yield strength of the ferritic matrix is raised by alloying, cleavage-initiation mechanisms other than carbide cracking are favored. At the same time, it should be noted that initiation mechanisms which require relatively high stresses to operate are not likely to produce many microcracks, inasmuch as the probability of propagation increases with the applied stress and one of the first few microcracks is liable to result in fracture before other microcracks can form. This, of course, means that "high stress" cleavage-initiation sources are less amenable to unequivocable identification than in the present case of carbide cracking.

Our description of the microcrack-initiation event due to carbide cracking is based on two premises:

(1) For cleavage to occur in ferrite, the normal stress on the cleavage plane must reach the critical value (i.e. cohesive strength of that plane) in less time than that required for plastic relaxation, either by dislocation multiplication and motion or by twin formation.

(2) The interface between alpha iron and Fe_3C is so strong that cleavage of the ferrite is energetically favored over the opening of the ferrite/cementite interface when the carbides crack.

The first point is self-evident, and the second is supported by the fact that the ferrite-cementite interface was never observed to break open in any of the specimens investigated.

Consider now the cracking of the carbide. In view of the fracture strengths measured by Webb and Forgeng (15) (6 to 12 x 10^5 psi for Fe_3C crystals), a stress concentration of more than a factor of 10 is required to account for the observed carbide cracks in the present work. This can be provided by a slip band or twin, as in Figures 1 and 8. Cracking of grain-boundary carbides may also result from the bending imposed on platelets of this brittle phase during plastic flow of the adjacent ferrite as the ferrite-carbide interfaces attempt to maintain continuity despite the surrounding shape changes. Since no significant amount of dislocation motion occurs in Fe_3C at or near room temperature (16), it appears that the carbides crack in an essentially brittle manner according to the Griffith energy

balance, without any plastic relaxation taking place in the carbide particle.

The surface energy of the cleavage plane of Fe_3C is not known, but on the assumption that it lies between 10^3 and 10^4 ergs/cm^2, Table III gives some estimates of the critical crack length in Fe_3C for applied stresses in the range of interest for the F4 ferrite, whose carbides are 3 to 10 μ in thickness. It can be seen that if the surface energy were 10^3 ergs/cm^2, most cracks in the carbides would be supercritical before reaching the adjacent ferrite, and would thus be propagating at a high velocity. On the other hand, if the surface energy were 10^4 ergs/cm^2, the critical length would be greater than the carbide thickness in most instances, and the crack within the carbide would have to propagate in a stable fashion, requiring continued widening of the initiating twin or slip band.

In either case, at the instant when the carbide crack has extended across the carbide thickness and reaches the ferrite, it will tend to act as a cleavage knife if a {100} plane of the adjacent grain is in fairly close registry with the plane of the carbide crack. If this condition is met, the response of the ferrite to this situation will be either (i) cleavage or (ii) plastic relaxation, as diagrammed schematically in Fig. 8. The probability of the latter response is greater at high temperatures, lower stress levels, and slower loading rates, but it also depends on the availability of dislocation sources in that region at that instant. Thus, the choice between local cleavage or plastic relaxation is a statistical event, even under fixed testing conditions. An indication of both responses occurring at cracks in the same carbide platelet is seen in Fig. 9. According to this concept of microcrack formation, a carbide crack causes cleavage in ferrite either at the instant it reaches the carbide-ferrite interface, or not at all. If the average cleavage strength of iron single crystals (3×10^9 dynes/cm^2) (8) and the approximate surface energy of iron (10^3 ergs/cm^2) are substituted in the Griffith equation,

$$\sigma = \left(\frac{2E\gamma}{\pi(1-\nu^2)c} \right)^{1/2} \qquad (1)$$

the critical crack length (2c) for initiating cleavage in the ferrite is about 3 μ. There are many carbides in the F4 ferrite large enough to give cracks of at least this length, but there are comparatively few in the F5 ferrite,* so an observable difference should appear

* The carbides in F5 are 1 to 3 μ in thickness.

in the propensity of microcrack initiation in the two materials, as is indeed the case.

In summary, if the ferrite adjacent to a cracked carbide cannot relax sufficiently rapidly, then the carbide crack behaves as a Griffith flaw with respect to the ferrite, and the criterion for microcrack initiation is given by the above equation. The conditions for subsequent propagation of the microcrack then depend on the continued suppression of plastic relaxation, as discussed in the following section.

3. Conditions for Fracture

In nonplastic solids containing pre-existing cracks, the fracture event usually comprises a single stage: that is, the long-range propagation of one of these cracks to failure. However, in most crystals, even though they may be relatively brittle, propagation is the second stage, the first being that of crack initiation through plastic deformation. Both events in metals require that a local stress reach a critical level in a time shorter than that taken by plastic deformation to relax the stress. Although both crack initiation and propagation are enhanced by increasing flow stress and strain rate and decreasing temperature, they are often separate events, particularly in the presence of "low stress" cleavage sources such as cracked carbides.

It is useful to consider the probability of cleavage fracture as being the product of two separate probabilities: initiation and propagation, i.e.,

$$P_F = P_I \times P_P \qquad (2)$$

and to examine the factors controlling each. Under given conditions of flow stress, strain rate and temperature, P_I and P_P depend, respectively, on the nature of the crack sources and paths available. As we have seen, crack sources can be of two types: (I) those which exist as a built-in distribution, such as carbides or brittle inclusions, and (II) those which arise through plastic deformation, such as twin or slip-band intersections. In the annealed F4 and F5 irons under study here, virtually all cleavage microcracks are initiated at type I sites. Consequently, it may be concluded that in this material, the activation of type II sites requires higher applied stresses or lower temperatures than do the type I sites. Table IV summarizes the factors which determine P_I for various crack sources, aside from considerations of stress, strain rate and temperature.

Once crack initiation has taken place, the question of whether fracture will occur becomes one of propagation. We consider first the case of continuous growth from the microcrack stage to final

fracture. In most studies of brittle fracture in single crystals, it has been found that $P_P \approx 1$ under conditions where P_I is finite. This, of course, is due to the absence of grain boundaries together with the concomitant misorientation of the cleavage planes in neighboring grains. For this reason, nonpropagating microcracks are rarely observed in iron single crystals, although a few have been detected by Honda et al (8), usually in cases where microcracks are blocked by mechanical twins.

Stated in terms of surface energy considerations, crack propagation in single crystals requires the expenditure of energy in the following forms: γ_s, true surface energy ($\approx 10^3$ ergs/cm^2 for iron); γ_p, the plastic-deformation energy required for dislocation motion and multiplication and cleavage-step formation, and γ_{tw}, the energy absorbed when the moving crack encounters a twin lying across its path. In polycrystals, a term γ_{gb} must be added to take account of grain-boundary barriers. The terms, γ_p, γ_{tw}, and γ_{gb}, reflect the tendency for plastic reflection in the matrix ahead of the crack front. They increase in magnitude with increasing density of mobile dislocations (ρ), with increasing temperature (T), and with decreasing crack velocity (V_c). Tetelman (17) has reported that γ_p varies as $\frac{\rho^{3/2} T^{5/2}}{V_c^2}$. γ_{tw} and γ_{gb} probably show the same kind of behavior, but may be several orders of magnitude greater than γ_p, depending on the misorientations of cleavage planes across the barriers involved. Thus, as the microcrack propagates through the ferrite, the γ_{tw} and γ_{gb} terms contribute energy peaks superimposed on a "background" of γ_s and γ_p.

Whether or not a moving crack is successful in overcoming the "friction" of γ_s and γ_p and the intermittent barriers of γ_{tw} and γ_{gb} will depend on the velocity of the crack. Following the development by Mott (18) and Roberts and Wells (19), Gilman (20) has used the idea of a critical crack velocity as the criterion for long-range crack propagation in a polycrystalline aggregate. By balancing the release of stored elastic energy with the energy absorbed by creation of new surface and the kinetic energy of the displaced material alongside the crack, the following expression is derived (18, 19, 20, 34)

$$\frac{V_c}{V_T} = 1 - \frac{2E\gamma_{eff}}{\pi\sigma^2 c} = 1 - \frac{c}{c^*} \qquad (3)$$

where V_c = velocity of the crack
V_T = terminal velocity of the crack (0.38 times velocity of sound)
σ = applied stress normal to the crack
c = half-length of the crack
c^* = half-length of the critical (Griffith) crack.

The variation of V_c with crack length is plotted in Fig. 10 according to Eq. (3).

It can be seen that variations in the effective γ become less important as the crack length increases and that beyond a certain length, which decreases with decreasing γ_{eff} and increasing σ (which corresponds to decreasing test temperature), continued propagation becomes almost a certainty.

At given values of σ and T, P_P depends on the grain size, twin density, and alignment of cleavage planes in the path of early-stage crack growth. It will be high, for example, in a single crystal with a $\langle 100 \rangle$ tensile axis or in a coarse-grained polycrystal with a pronounced $\langle 100 \rangle$ texture. In a polycrystalline aggregate, each localized group of grains offers a propagation path which will be more or less difficult depending on the above factors. In other words, a microcrack is more likely to result in fracture of the specimen if it forms as a part of a low-resistance path. In Fig. 11, for example, the microcrack which initiates at C is more dangerous to the specimen than those which form at A and B.

At test temperatures just below T_d where many microcracks form before fracture, both P_I and P_P are important in determining P_F. However, as γ_{eff} decreases and σ increases with lower temperatures, the resistance of all paths decreases, and P_P approaches unity. Finally, at very low temperatures, e.g. $\sim -195^\circ$C for F4, P_I alone controls P_F, and no arrested microcracks are found.

As far as the ferrite matrix of F4 and F5 is concerned, P_P can be regarded as the same for both materials, in view of the marked similarity in yield stress (Fig. 6), grain size (Table I), twinning behavior (Fig. 7), and strain-hardening behavior (Fig. 12). The great difference in their low-temperature fracture properties, as illustrated in Fig. 12, is due to the difference in carbide content and thickness. Initially, the curves are alike for each temperature; however, P_F is large enough in F4 for cleavage to occur before necking at the four test temperatures shown. In F5 at -120°C, P_I is essentially zero because the flow stress is too low for cracks in the thin carbides to be effective, and the specimen is very ductile. At the two intermediate temperatures, P_I becomes finite, but the number of microcracks formed is still small; hence, the probability of one forming in a low-resistance path is low, leading to a low P_P. Below -160°C, the flow stress level becomes high enough to give sizable values of P_I and P_P, and cleavage fracture then precedes the formation of a neck.

It should be emphasized that the microcrack which starts the final fracture in these ferrites need not propagate continuously from a carbide crack. Fracture may well be triggered by an arrested microcrack which is reactivated at a higher stress level. However,

since the stopped microcrack originally came from a carbide, P_I (and therefore P_F) will still depend on the amount of carbide as outlined above.

In the tensile-property curves shown in Fig. 6, we note that the cleavage stress of the F5 ferrite is appreciably higher than that of F4 in the temperature range -160 to -195°C. Otherwise, the fracture behavior of the two ferrites appears to be qualitatively similar, except that the low T_d for F5 obscures any such rise in cleavage stress as exhibited by F4 on decreasing temperature between -90 and -160°C. The higher cleavage stress observed in F5 is believed to be connected with the lower rate of production of microcracks in this material with increasing plastic strain as denoted by Fig. 5. The upper curve gives the number of cracks versus strain for two F4 specimens, each tested at a different temperature below T_d. Both specimens follow the same curve, indicating that plastic strain is the important variable, not temperature (as long as it is below T_d). Similar data for an F5 specimen tested at -180°C are given by the lower curve. It is clear that increasing strain produces microcracking in the F5 ferrite at a much-reduced rate, due to the lower carbide content. We therefore expect a longer strain-hardening range before fracture in F5 than in F4 since, if P_I is low, a general raising of P_p through strain hardening is required to attain a fracture probability comparable to that of F4 at any given test temperature.

In both materials at sufficiently low test temperatures, there is a decrease in fracture stress with decreasing temperature. This phenomenon is related to the fact that twinning begins to supersede slip as the dominant mode of deformation at these temperatures.

4. Effects of Twins on the Brittle Behavior of Iron

The role of twins in the low-temperature fracture of F4 ferrite has been studied in two ways: by suppressing the twinning with a 3 percent prestrain at room temperature, and by increasing the twin density with prestrains of about 0.5 percent at -160 or -195°C. (21, 22) For the first pretreatment, T_d remains essentially unchanged, but the cleavage stress is lowered (Fig. 13) due partly to the increase in flow stress produced by prestraining and partly to the fact that twins can raise the cleavage-fracture stress by reducing the low-resistance paths for crack propagation, i.e., by decreasing the effective grain size. The same effect has been observed in zinc single crystals (23).

A much more striking result is obtained, however, when a very high initial twin density is generated by prestraining at low temperatures (pretwinning). Fig. 14 shows the effect of prestraining 0.5 percent at -160°C on the subsequent tensile behavior at -110°C (20°C below T_d for annealed F4); this is compared with specimens

having prestrains of zero percent and 3 percent at room temperature. It is found (22) that pretwinning at -195°C causes a lowering of T_d to about -160°C, as indicated by the reduction in area curves of Fig. 15; this effect is connected with a pronounced suppression of microcrack formation at temperatures above approximately -150°C. Below this temperature, microcracking is essentially unaffected by the pre-existing twins. This influence of pretwinning on microcrack initiation and the concomittant lowering of T_d are probably the result of:

(i) additional modes of stress relaxation afforded by the high lateral mobility of the twin-matrix interfaces, (24) and
(ii) partitioning of grains by twins, leading to a decrease in the length of slip bands impinging on carbides and thus reducing the tendency for carbide cracking.

Apparently, these effects of pretwinning manifest themselves mainly in coarse-grained materials with high T_d, since the Charpy impact transition temperature of a coarse-grained rimmed steel could be lowered by about 20°C by pretwinning, (25) while that of a fine-grained killed steel was virtually unchanged (22). This behavior is not unexpected, inasmuch as Fig. 15 indicates that the ability of pre-existing twins to inhibit microcracking disappears at low testing temperatures, thus suggesting that materials with relatively low T_d will not be benefited by the pretwinning.

5. Ductile Fracture

In the polycrystalline ferrites under study here, the carbides also play an important role in the ductile fracture. Fig. 16 gives some examples of large voids which are characteristically found in the necked regions of F4 tensile specimens. These voids are generated from carbide cracks under the influence of hydrostatic stresses in the neck, and their size increases with the extent of necking, as seen in Fig. 17. The voids provide paths of weakness through which fracture can travel by the rupture of the intervening material, whether by cleavage or by fibrous tearing. Consequently, they behave in much the same manner as the voids formed around inclusions in the ductile fracture of copper (26). Fig. 18 demonstrates that the voids developed in the F5 ferrite are much fewer in number and smaller in size than those in F4, even in a specimen which has undergone a larger reduction of area. This difference in ductile fracture between the F4 and F5 materials is directly a function of the carbides present.

The effect of the void formation on the tensile properties is evident from Fig. 6. The F4 ferrite undergoes less reduction in area above the transition temperature than does F5, and this is reflected in a much lower fracture stress. It should be noted, however, that the fracture stress used here is simply the load at fracture divided by the area of the fracture. In necked specimens, this value does not represent a true flow stress, as does the fracture stress below

T_d; it was not thought worthwhile for present purposes to apply a correction of the Bridgman-type for these flat specimens.

6. The Transition Temperature

Cleavage fracture can occur after necking at temperature just above T_d and is then triggered by the expansion of voids. As the test temperature is lowered toward this level, the ability of the specimen to tolerate void expansion lessens, and the reduction in area decreases along with the percentage of fibrous fracture. When cleavage fracture (initiated by the carbide-cracking mechanism) takes over before necking occurs, this temperature is designated as T_d and denotes the onset of brittle behavior, but not nil-ductility. In essence, T_d is the temperature below which the fracture strain and uniform strain become identical. Below T_d, the ductility gradually decreases to nil with decreasing temperature. The temperature at which this occurs has been denoted by some authors, e.g. (4, 5), as the brittle transition temperature (T_b). This corresponds to the temperature below which fracture occurs during the initial yielding, but does not involve a transition from fibrous to cleavage, since the fracture is already completely cleavage above this temperature. T_d is more closely related to the transition from fibrous to cleavage fracture, but there is still no one-to-one correlation. Fracture becomes fully cleavage at T_d in certain mild steels (1), just above T_d in the present materials, and well above T_d in molybdenum (27). The ductility transition, as denoted by T_d, appears to be determined mainly by whether the plastic instability corresponding to necking sets in before fracture takes place; a relatively large reduction of area accompanies the plastic instability, and any factor which inhibits the latter tends to raise T_d.

On the other hand, the transition in fracture mode is affected by the details of cleavage initiation in the particular material, as we have shown here. Since the factors controlling the fracture-mode transition and the ductility transition are not necessarily directly coupled, it is not surprising to find that they often occur in somewhat different temperature regions.

7. Intergranular Fracture

In view of the fact that carbide cracking is the dominant mode of cleavage initiation even in very low-carbon ferrite, it is of interest to examine the behavior of the F5 ferrite in the absence of precipitated carbides. To this end, specimens which had been given the original annealing heat treatment (Table 1) were reheated to 705°C, quenched, and tested at -195°C. A priori expectations were to find a ductility greater than the 3 to 5 percent elongation observed in the slowly cooled samples. Instead, the quenched specimens exhibited extreme brittleness, fracturing after essentially no plastic strain. The only evidence of plastic strain prior to fracture consisted of scattered patches of twinned grains distributed

over the gauge section. It turned out that the quenching treatment had altered the mode of fracture from almost entirely cleavage or transgranular (TG) in the slowly cooled specimens to mostly intergranular (IG) in the quenched samples. An example of the latter is seen in Fig. 19.

Low and Feustel (28) have shown that a similar kind of grain-boundary embrittlement occurs at -195°C in mild steel after decarburization in wet hydrogen, and that the grain-boundary cohesion can be restored by recarburizing. This effect is evidently connected with the amount of carbon at grain boundaries. Acting on the premise that a similar phenomenon might be operating in the quenched F5 specimens, experiments were carried out to determine the influence of quenching temperature on the fracture characteristics (29), since the amount of dissolved carbon localized at grain boundaries can be controlled by the extent of equilibrium segregation which occurs in the alpha region (30).

The quenching treatments are summarized in Fig. 20. After the initial anneal, specimens were reheated well into the alpha region (705°C) and either quenched to -195°C, via iced brine, or furnace-cooled to some temperature T_Q and quenched as before.

The results of the tensile tests at -195°C and of the metallographic examinations of the fracture surfaces and specimen faces are given in Fig. 21. As T_Q is lowered from 705°C to about 600°C, the amount of twinning before fracture increases, but the total fracture strain remains very small. Twin-induced intergranular microcracks are first detected in this range, and the number of these IG microcracks increases with the amount of twinning as T_Q is lowered, reaching a maximum at about T_Q = 570°C. At the same time, the proportion of IG fracture (percentage of IG facets) drops continuously as T_Q is lowered, and the fracture strain (percent elongation to fracture) increases. Below T_Q= 570°C, the number of IG microcracks decreases, indicating that the grain boundaries are now better able to withstand the impact of twins; at this point, the strain to fracture begins to increase, and attains a maximum value of 15 percent elongation. At about T_Q = 480°C, precipitated carbides are first observed, and this is accompanied by the appearance of TG microcracks. Below T_Q = 400°C, IG microcracks are no longer observed; the specimens fracture after about 1 to 5 percent elongation, mainly by the TG mode, and they contain carbide-initiated TG microcracks

It is important to note that these variations in fracture behavior with quenching temperature are essentially reversible. For example, the relatively high ductility corresponding to T_Q = 480°C is lost if the specimen is reheated to 705°C and quenched. Furthermore, re-equilibration at a lower temperature will restore the ductility. Accordingly, the observed changes in mode of fracture cannot be attributed to gain or loss of carbon or oxygen during the heat treatment.

An example of one of the twin-initiated IG microcracks is given in Fig. 22. Most of these grain-boundary microcracks were observed to have been initiated in the manner shown. They always lie on one side of the twin: the side on which the twinning shear acts to wedge-open the boundary. Therefore, the predominant initiation mechanism for IG cracking is simply a slight modification of the classical Zener mechanism (2). Similar observations in chromium, molybdenum and tungsten have recently been reported by Gilbert et al (31).

The intergranular-strengthening effect which occurs when T_Q is lowered from 705°C to about 480°C is believed to be due to the equilibrium segregation of carbon to the grain boundaries. When specimens are quenched from temperatures high in the alpha region the carbon is distributed more uniformly throughout the grains, and the cohesive strength of grain boundaries could then become low for either of the following reasons:

(i) the grain boundaries in iron may be surfaces of inherent weakness but are strengthened by certain segregated impurities such as carbon; or

(ii) the grain boundaries in the F5 ferrite may be weakened by the presence of an element (presumably oxygen) which remains segregated at the grain boundaries of the ferrite even at the higher quenching temperatures, but whose deleterious effect can be offset by a sufficient concentration of carbon.

The strengthening of the ferrite crystals by the quenched-in supersaturation of carbon undoubtedly contributes to the intergranular-fracture phenomena observed after the high-temperature quenching, since plastic relaxation in response to a twin impinging on the grain boundary is inhibited; however, the results of Low and Feustel (28) clearly show that this is not the controlling factor in the grain-boundary weakening.

It is not unreasonable to suppose that the grain boundaries of an ultrapure polycrystalline metal may provide surfaces of inherent weakness, at least in certain temperature ranges, due to the extended atomic bonds across the interfaces. Under such conditions, the grain boundaries could be strengthened if the extended M-M bonds are replaced by strong M-X-M complexes. Carbon may well play this type of role in segregating to the grain boundaries if T_Q is lowered toward the solvus temperature.

On the other hand, oxygen (among other elements) has long been suspected as a source of grain-boundary weakness in iron and other transition metals, and it is possible that the 20 PPM residual oxygen acts in this way in the F5 ferrite. Oliver and Garofalo (32) have shown that carbon and oxygen in the 5 to 20 PPM range in high-impurity iron can interact to immobilize each other. If such an interaction occurs along the grain boundaries in iron as T_Q is lowered, this could result in a strengthening of the grain boundaries, conceivably through the replacement of Fe-O-Fe complexes by Fe-C-Fe complexes.

However, at the present time, one cannot decide on the exact origin of the intergranular weakness in polycrystalline iron. Nevertheless, the counteracting effect of carbon, in this respect, is becoming increasingly clear.

Although we have dealt here exclusively with polycrystalline materials, it may be well to emphasize that similar grain-boundary phenomena have been observed in the cleavage fracture of single crystals! Honda et al (8) have shown that iron single crystals grown by the strain-anneal technique invariably contain microscopic occluded crystallites, and that cleavage fracture is often initiated at cracks at the boundaries of these artifacts. This effect seems to be especially prevalent when the crystals have a high oxygen content, which may be an unfortunate consequence of the use of wet hydrogen for decarburizing during sample preparation.

8. Summary

A critical investigation has been undertaken concerning the various modes of fracture initiation and propagation that operate on a microscale in polycrystalline iron. Particular emphasis is placed on the micromechanisms of cleavage initiation and the relevance of such phenomena to the ductile-brittle transition.

In polycrystalline ferrites of comparatively high purity and carbon contents down to 0.005 percent, the main source of cleavage microcracks at test temperatures near or below the ductility-transition temperature is the cracking of grain-boundary carbides when the specimens undergo general plastic deformation. Except for single crystals and extremely coarse-grained polycrystals, neither slip-band nor twin-band intersections play an important part in the cleavage-initiation process, at least at temperatures down to -195°C. The carbide cracks act as Griffith flaws in promoting cleavage of the ferrite, but do so only at the instant of their formation. The probability of ferrite cleavage resulting from a carbide crack increases with increasing carbide thickness and decreasing temperature.

It appears that mechanical twinning becomes a factor in cleavage initiation when the flow-stress is increased, as in solid-solution hardening by silicon or phosphorus, or alternatively when the grain size is increased, especially in the limiting case of single crystal specimens.

If carbides in a low-carbon ferrite are re-dissolved by quenching from a high solution temperature, extreme brittleness is observed at -195°C due to the incidence of grain-boundary failure. However, when the quenching temperature is lowered toward the solvus line, the strain to fracture increases sharply and the intergranular fracture diminishes, presumably because of an increasing equilibrium segregation of carbon to the grain boundaries. A ductility maximum on testing at -195°C occurs when the iron is quenched from the vicinity of the solvus temperature, in that the

precipitation of the cleavage-initiating carbides takes place on equilibration at lower temperatures. The intergranular mode of fracture initiation is also operative in single crystals of iron because occluded grains are usually present, and the resulting internal boundaries can become sites for fracture initiation.

The barriers to microcleavage propagation in polycrystalline iron are, in order of decreasing effectiveness: (a) grain boundaries, (b)pre-existing mechanical twins, and (c) initiation of slip bands and/or twins at the tip of the advancing crack. (See Ref. 11, Table III) Another important structural factor lies in the statistical distribution of crystallographic orientations of the grains; the propagation process is favored in those regions having a chance alignment of easy cleavage paths.

As the test temperature is raised above the ductility transition, carbide cracking still takes place when plastic deformation of the ferrite occurs, but such cracks then lead to the formation of cavities instead of cleavage cracks. These voids can become relatively large during the necking stage of a tensile specimen, and eventual tearing or shearing between the voids results in the characteristic fibrous or shear fracture. Thus, the cracking of carbides (or other brittle phases) constitutes an important source of initiation sites for ductile as well as brittle fracture.

Although the ductility-transition temperature, as observed in the tensile test, is related to the interplay of these various modes of fracture, the transition temperature itself has a mechanical basis; it is the temperature below which the fracture precedes the formation of a neck, i.e., the fracture strain then becomes equal to the uniform strain. Hence, while there is usually a conspicuous decrease in ductility when the test temperature passes from above to below this transition temperature, the ductility does not drop to zero at this point. It requires further lowering of the test temperature before the fracture occurs during the initial yielding or twinning process which then corresponds to a condition of nil ductility.

Acknowledgements

The authors wish to express their appreciation to Dr. R. Honda and Mr. B. Rosof for valuable discussions and for making available the results of unpublished research. Messrs. R. C. Whittenmore and B. Rosof and Miss M. Yoffa assisted with the experiments. Financial support was received from the Ship Structure Committee under Contract Nobs-88279 at the Massachusetts Institute of Technology and the Advanced Research Projects Agency at the University of Pennsylvania.

References

1. G. T. Hahn, B. L. Averbach, W. S. Owen, and M. Cohen, Fracture, p. 91, Wiley, New York (1959).

2. C. Zener, Fracturing of Metals, p. 3, ASM, Cleveland (1948).

3. N. J. Petch, J. Iron Steel Inst., 174 (1953) 25.

4. A. N. Stroh, Advances in Phys., 6 (1957) 418.

5. A. H. Cottrell, Trans. Met. Soc. AIME, 212 (1958) 192.

6. D. Hull, Fracture of Solids, Interscience, p. 417 New York (1962).

7. R. Honda, J. Phys. Soc. Japan, 16 (1961) 1309.

8. R. Honda, M. Cohen, B. L. Averbach, to be published.

9. T. L. Johnston and E. R. Parker, Fracture of Solids, p.267 Interscience New York (1962).

10. J. R. Low, Relation of Properties to Microstructure, p. 163 ASM, Cleveland (1954).

11. C. J. McMahon, Jr. and M. Cohen, Acta Met., 13 (1965) 591.

12. W. H. Bruckner, Welding Journal-Research Supplement 29, (1950) 467S.

13. N. P. Allen, W. P. Rees, B. E. Hopkins and H. R. Tipler, J. Iron and Steel Inst., 174 (1953) 108.

14. C. N. Reid, A. Gilbert and G. T. Hahn, ASD-TDR-63-360, April (1964).

15. W. W. Webb and W. D. Forgeng, Acta Met., 6 (1958) 462.

16. A. S. Keh, Acta Met., 11 (1963) 1101.

17. A. S. Tetelman, Fracture of Solids, p. 461 Interscience, New York (1962).

18. N. F. Mott, Engineering, 165 (1948) 16.

19. D. K. Roberts and A. A. Wells, Engineering, 178 (1954) 820.

20. J. J. Gilman, J. Appl. Phys., 27 (1956) 1262.

21. B. Rosof, B. S. Thesis, M.I.T., Cambridge (1963).

22. B. Rosof, M. S. Thesis, M.I.T., Cambridge (1964).

23. M. Gensamer, Trans. Met. Soc. AIME, 215 (1959) 2.

24. R. Honda, Private Communication.

25. C. J. McMahon, Jr. unpublished research.

26. K. E. Puttick, Phil. Mag., 4 (1959) 964.

27. B. S. Lement, D. A. Thomas, S. Weissmann, W. S. Owen and P. B. Hirsch, ASD-TR-61-181, Part III, p. 67, April (1963).

28. J. R. Low and R. G. Feustel, Acta Met., 1 (1953) 185.

29. C. J. McMahon, Jr., Acta Met., in press.

30. D. McLean, Grain Boundaries in Metals, p. 116, Oxford (1957).

31. A. Gilbert, G. T. Hahn, C. N. Reid and B. A. Wilcox, Acta Met., 12, (1964) 754.

32. B. F. Oliver and F. Garofalo, Trans. Met. Soc. AIME, in press.

33. R. P. Smith, Trans. Met. Soc. AIME, 224 (1962) 105.

34. E. N. Dulaney and W. F. Brace, J. Appl. Phys., 31 (1960) 2233.

TABLE I

Materials and Treatments Used

Material	Composition (Wt.%) C	N	O	Other	Heat Treatment	Average Grain Diameter (mm)	ASTM Grain Size Number	Tensile-Ductility Transition Temperature T_d
Ferrite F4	0.035	0.0004	0.0017	<0.045	1250°C-4hr.-F.C.	0.32	0.7	-90°C
Ferrite F5	0.005*	0.0002	0.0020	<0.082	925°C-4hr.-F.C.	0.25	1.4	-160°C

F.C. = Furnace-cooled (2-3°C per minute)

* This value was previously reported as 0.007 (11), but since shown to be 0.005%.

TABLE II

Sources of Surface Microcracks in F4 and F5 Ferrite

Specimen	F4	F4	F5
Tensile test temperature	-140°C	-180°C	-170°C
Total number of microcracks observed per 10,000 grains	66	43	17
Number of microcracks originating at cracked carbides	63	42	12
Origin of microcracks not certain--probably cracked carbides	3	1	4
Origin of microcracks not certain--possibly twin-matrix interface	0	0	1

TABLE III

Length of Critical (Griffith) Crack in Fe_3C

Applied Stress (psi)	γ (ergs/cm^2)	2C(u)
35,000	10^3	4.6
	10^4	46
80,000	10^3	0.9
	10^4	9

Table IV

Factors which Influence Probability of Crack Initiation for Various Crack Sources.

Type of Crack Source	Factors which Increase P_I
Type I	
brittle inclusion	Increasing thickness of platelet
	Increasing number in population
Type II	
twin/twin or twin/grain-boundary intersection	Increasing grain size (length, thickness and velocity of moving twin)
	Increasing degree of ⟨100⟩ tensile-axis texture
slip/slip or slip/grain-boundary intersection	Increasing rate of formation of slip band (high dislocation velocity and rate of multiplication, low ability to cross slip)
	Increasing grain size

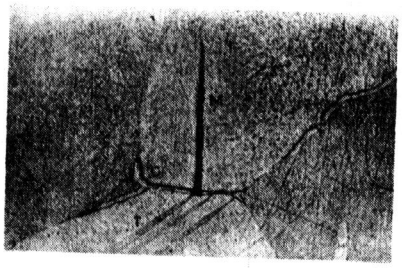

Fig. 1.

Example of a cleavage microcrack M initiated at grain-boundary carbide C which was cracked by impingement of twin T. F4 ferrite tested at -180°C, repolished surface. Tensile axis horizontal. 360X (Ref. 11)

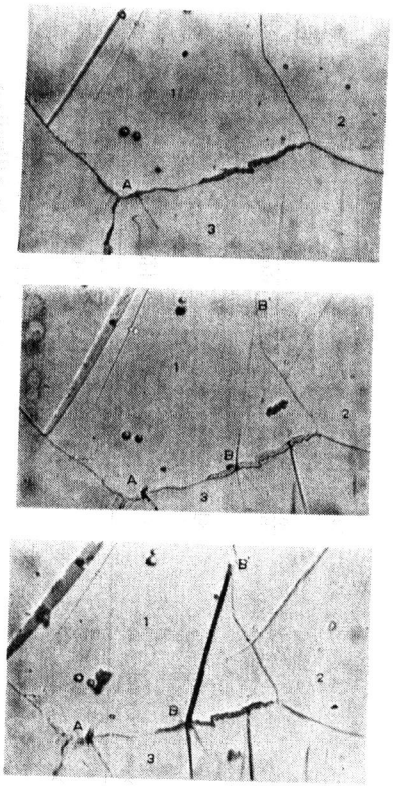

(a) First loading step. Crack in carbide at A has initiated twins in grain 3.

(b) Second loading step. More carbide cracks have initiated twins in grain 3 at B and C and a microcrack BB' in grain 1.

(c) Third loading step. Microcrack BB' has opened.

Fig. 2 Stages of microcrack formation in F4 specimen tested at -180°C (See Fig. 3). Tensile axis horizontal. (Ref. 3).

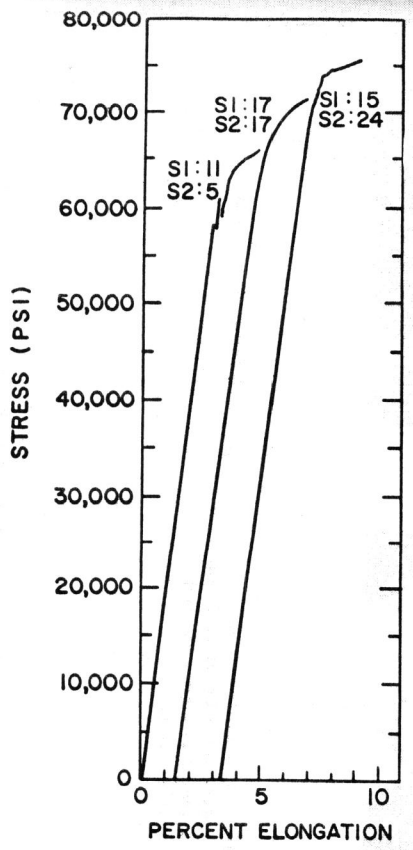

Fig. 3 Stress-strain curves for interrupted tensile test of F4 ferrite at -180°C. Numbers refer to new microcracks formed during each loading cycle on the two side faces of the specimen. (Ref. 11)

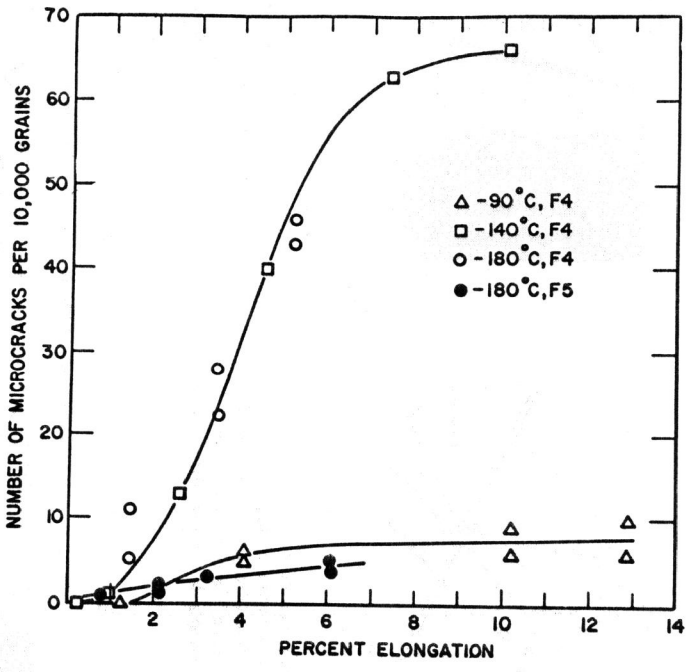

Fig. 5 Effect of plastic strain on the number of surface microcracks in tensile specimens tested in interrrupted-loading. (Ref. 11)

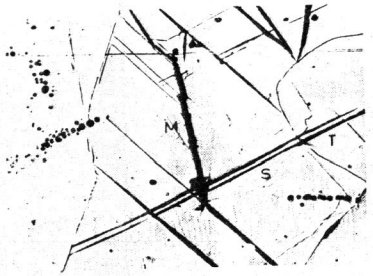

(a) Specimen surface. Microcrack M has no apparent connection with a carbide. Bands marked T are twins, while those marked S are slip. 125X

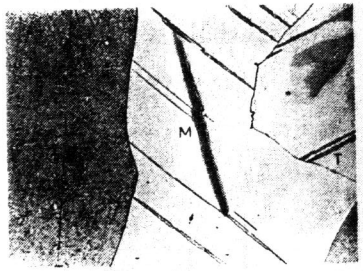

(b) After removing one mil from surface, slip bands have disappeared. 125X

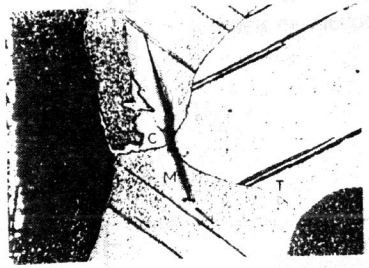

(c) One more mil removed. Large cracked carbide C now revealed as the microcrack source. 125X

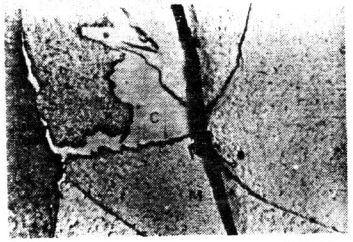

(d) Same as (c) 310X

Fig. 4 Exposure of microcrack source lying below the surface of an F4 specimen tested at -180°C. Tensile axis horizontal. (Ref. 11)

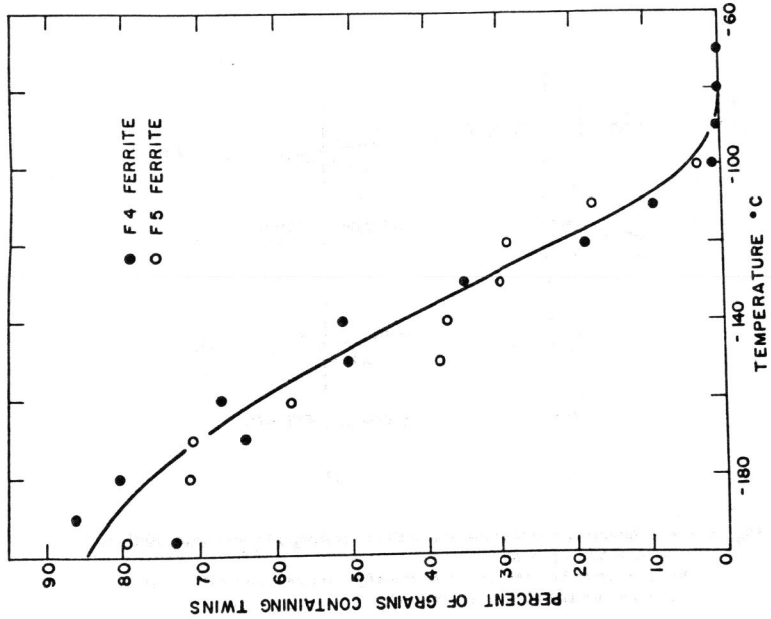

Fig. 7 Influence of tensile test temperature on the amount of generally distributed twinning in specimens pulled to fracture. (Ref. 11)

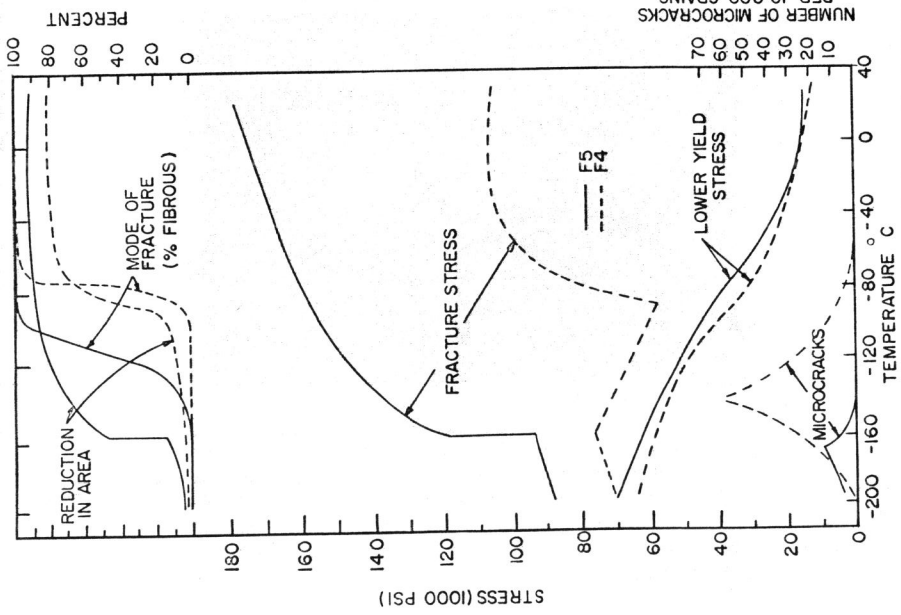

Fig. 6 Comparison of tensile properties and microcracking tendency of F4 and F5 ferrite.

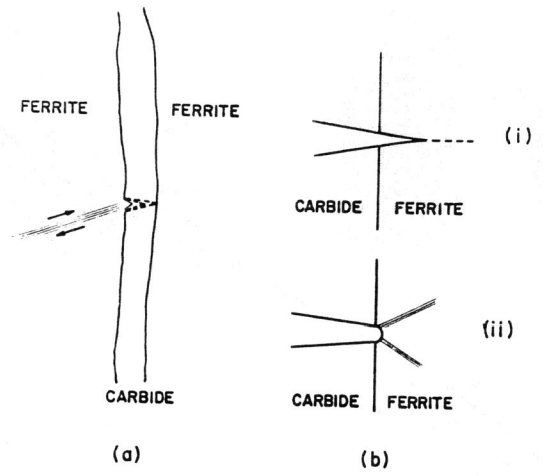

Fig. 8 (a) Schematic representation of the cracking of a carbide platelet by a twin or slip band.
(b) Two possible responses of the adjacent ferrite: either (i) cleavage, or (ii) plastic relaxation.

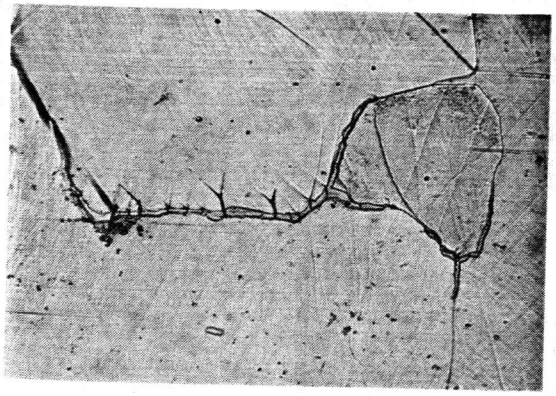

Fig. 9. Example of multiple cracking of a grain-boundary carbide which has led to both cleavage and plastic deformation of the adjacent ferrite. 200X (Ref. 11)

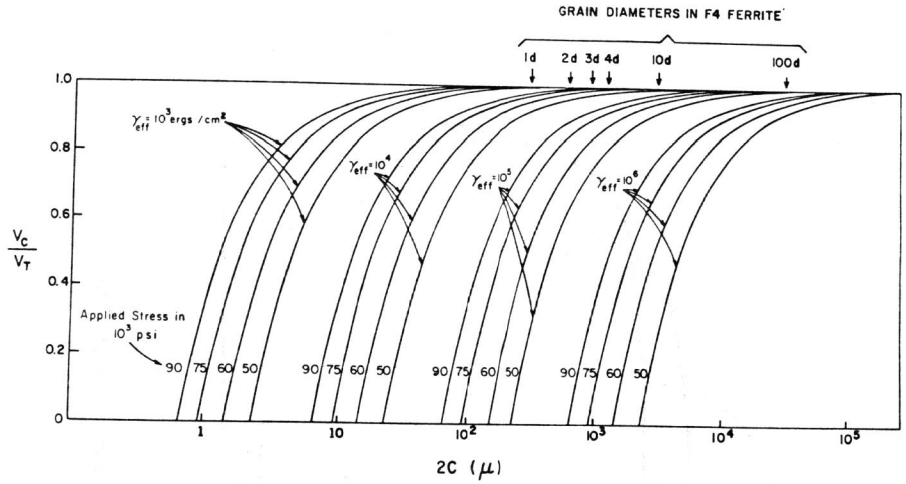

Fig. 10 Crack velocity versus crack size for various conditions of applied stress and effective surface energy.

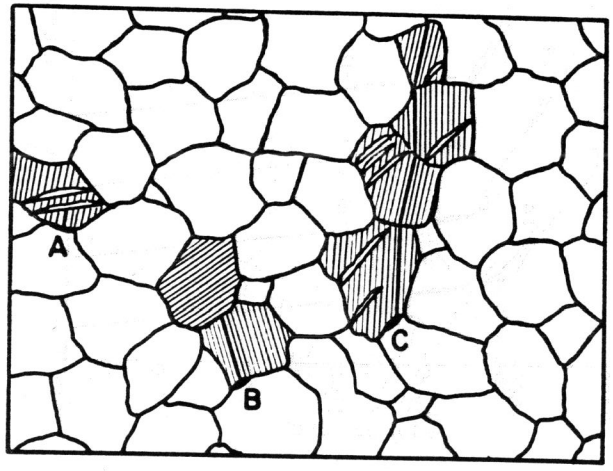

Fig. 11 Paths of varying degrees of resistance to early-stage crack propagation. Microcrack A stopped by twin; microcrack B stopped by boundary of grossly misoriented grain; microcrack C encounters no strong barriers and leads to fracture.

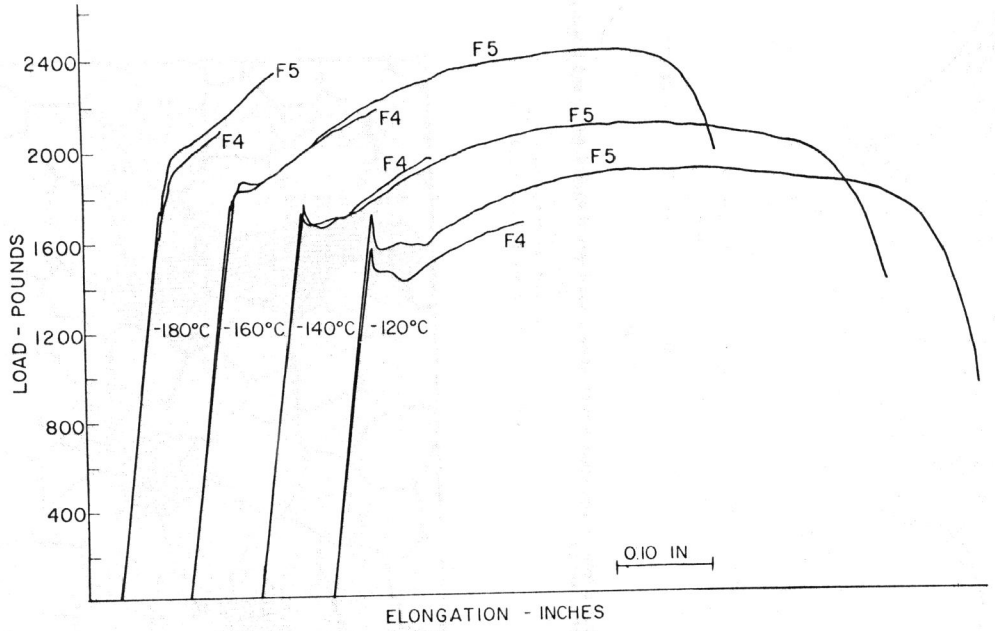

Fig. 12 Examples of load-elongation curves of F4 and F5 ferrite. (Ref. 11)

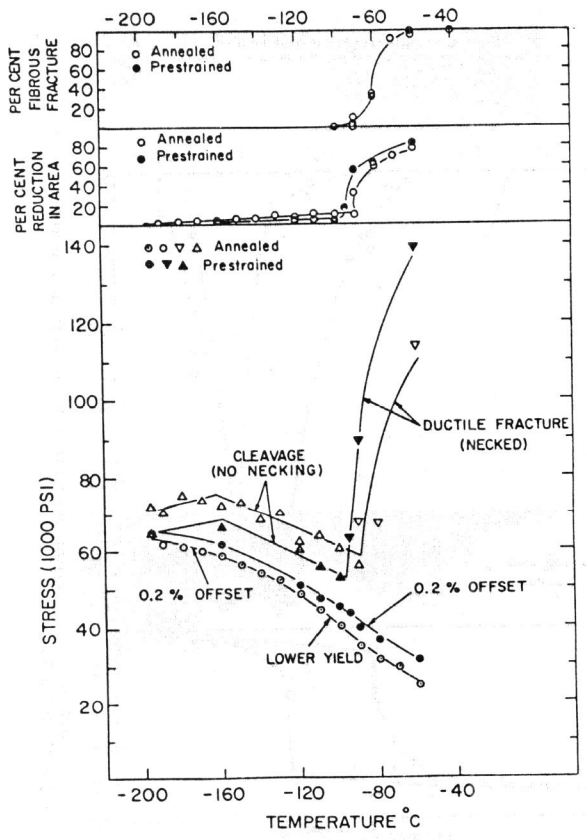

Fig. 13 Effect of 3 percent prestrain at room temperature on the fracture characteristics of F4 ferrite (Ref. 11)

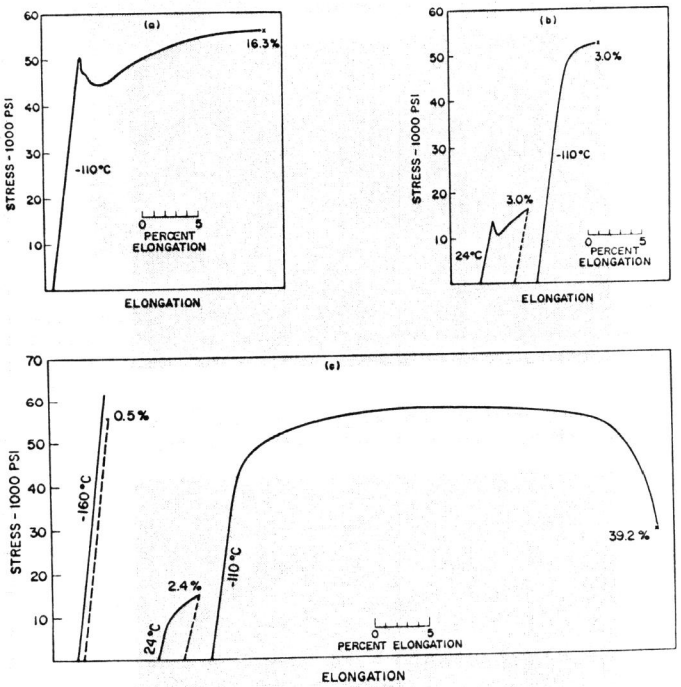

Fig. 14 Stress-strain curves of F4 ferrite tested at -110°C. (a) with no prior mechanical treatment; (b) with 3.0% prestrain at room temperature; (c) with 0.5% prestrain at -160°C, and 2.4% prestrain at room temperature. (Ref. 21)

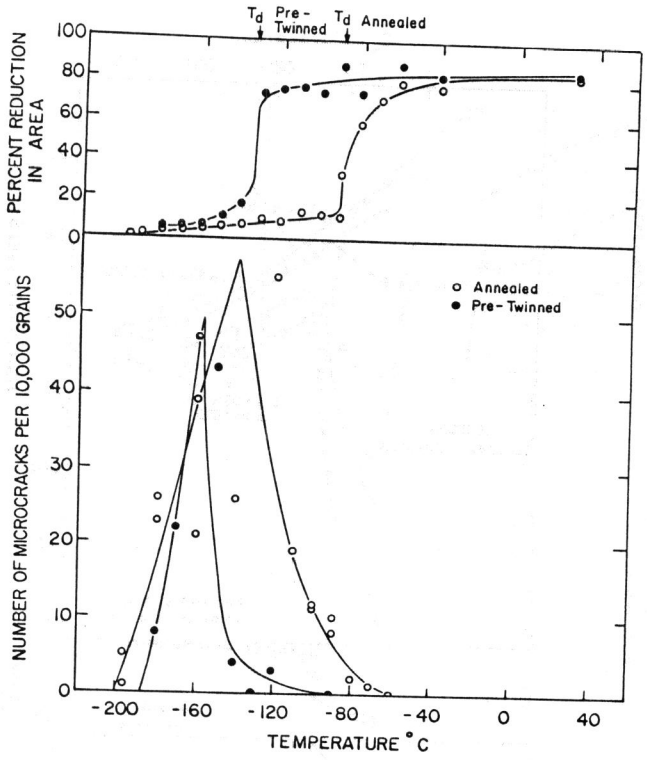

Fig. 15 Effect of pretwinning on microcrack formation and on the ductility transition in F4 ferrite. (Refs. 11 and 22).

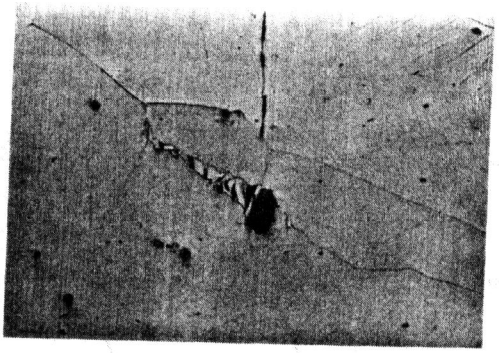

(a) Voids from cracked carbide in neck of F4 specimen near fracture. 32.3% reduction in area. Tested at -90°C.

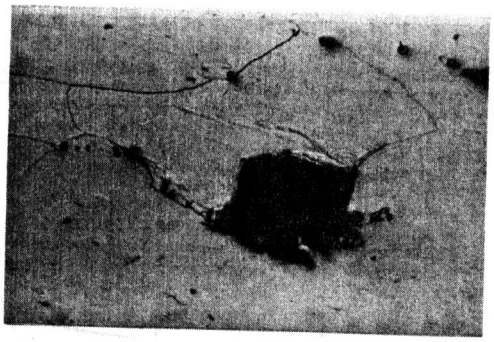

(b) Large void from cracked carbide in neck of F4 specimen near fracture. 70.0% reduction in area. Tested at -70°C.

Fig. 16 Voids generated from cracked carbides in neck of F4 specimens. Ground approximately to half-thickness. Tensile axis horizontal. **170X**

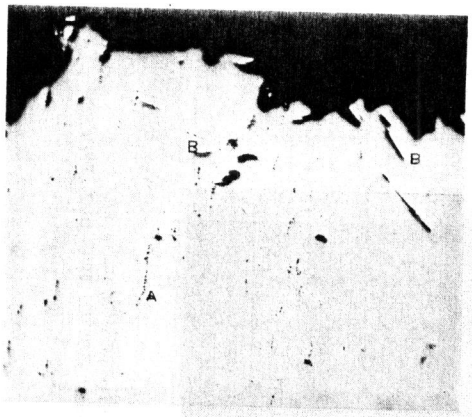

(a) Voids in neck of F4 specimen at fracture. 32.3% reduction in area. Note cracked carbides at (A) and cleavage cracks at (B). Fracture about 10% fibrous. Tested at -90°C.

(b) Voids in neck of F4 specimen at fracture. 58.4% reduction in area. Fracture about 35% fibrous. Tested at -80°C.

(c) Voids in neck of F4 specimen at fracture. 70.0% reduction in area. Note increase in size of holes from cracked carbides as strain in the neck increases. Fracture about 95% fibrous. Tested at -70°C.

Fig. 17. F4 specimens ground approximately to half-thickness, unetched. Tensile axis vertical. 35X.

Fig. 18. Neck of F5 specimen at fracture, showing only a few small voids. 83.0% reduction in area. Longitudinal cleavage crack at (A). Fracture about 60% fibrous. Tested at -110°C. Ground approximately to half thickness. Unetched. Tensile axis vertical. 35X

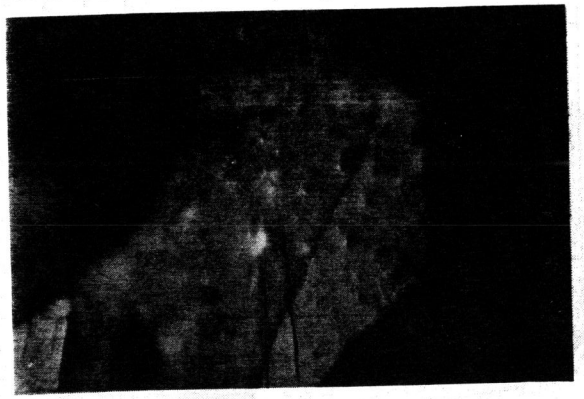

Fig. 19 Example of intergranular fracture facets in F5 ferrite quenched from 705°C and tested at -195°C. 500X (Ref. 29)

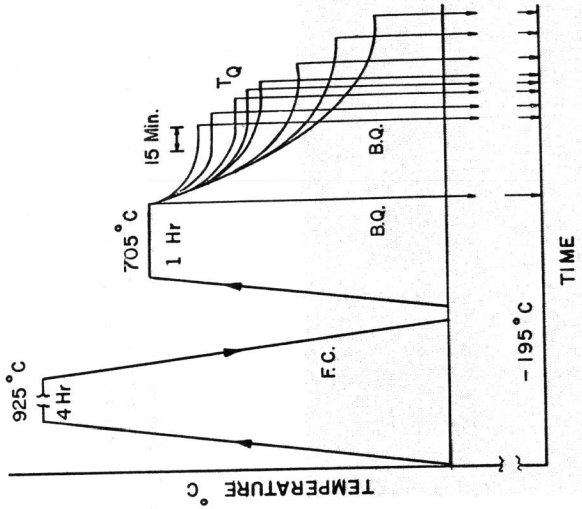

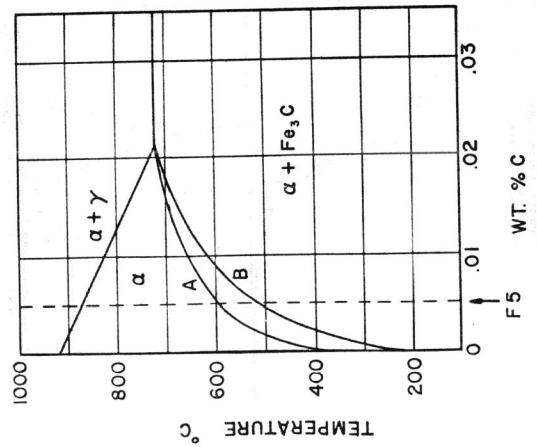

Fig. 20 (a) Solubility of carbon in α iron: A-thermodynamic data of Smith and Stanley, B-anelastic data of West, Dijkstra, and Lindstrand. (Ref. 33)
(b) Schematic representation of heat treatments on F5 ferrite. F.C. = furnace cool; B.Q. = brine quench; T_Q = equilibration temperature prior to quench. (Ref. 29)

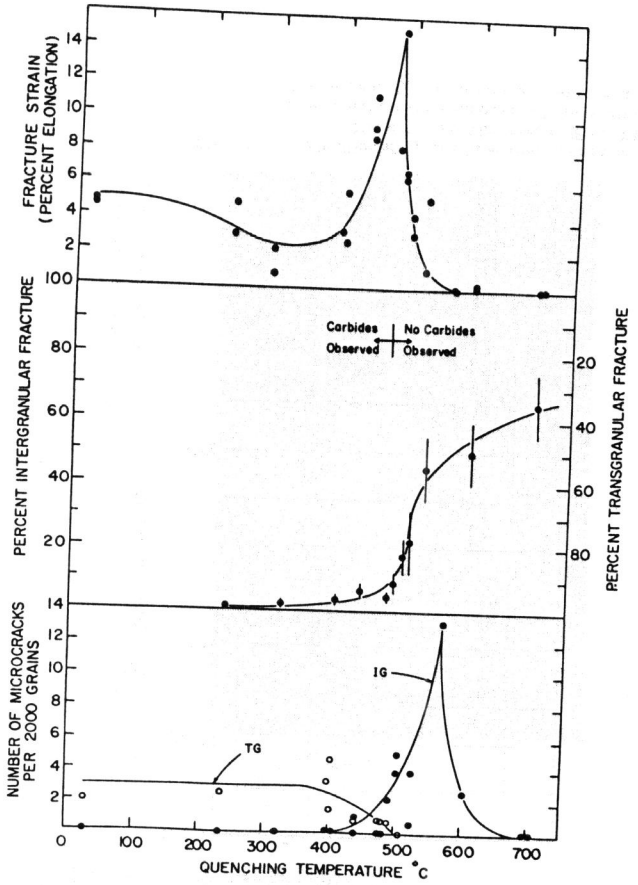

Fig. 21 Influence of quenching temperature on the fracture characteristics of F5 ferrite tested -195°C. (Ref. 29)

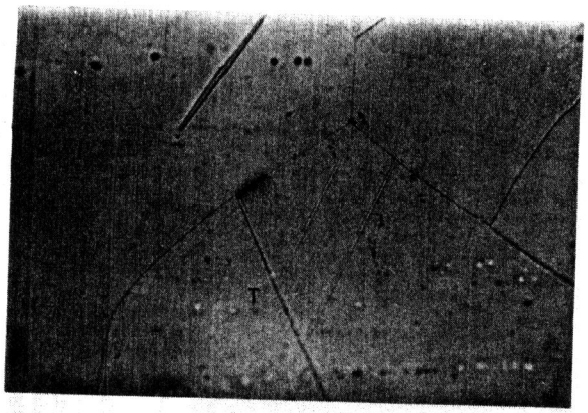

Fig. 22 Example of an intergranular microcrack in F5 ferrite quenched from 525°C, initiated by twin T. Tensile axis horizontal. 500X (Ref. 29)